ORIGINAL RESEARCH

Derivatives of benzo[b]furan. Part I. Conformational studies of khellinone and visnaginone

**Tomas Pena Ruiz · Aleksandra Drzewiecka ·
Anna E. Koziol · Manuel Fernandez Gomez ·
Kinga Ostrowska · Marta Struga · Jerzy Kossakowski**

Abstract The structural analysis of khellinone and visnaginone indicated the planarity of the benzo[b]furan ring system. The oxygen or carbon atoms of the substituents, –OH, –OCH$_3$, and –C(=O)CH$_3$, are nearly coplanar with the aromatic ring. The molecular conformation is stabilized by the intramolecular O–H···O hydrogen bond formed between the *ortho*-substituted hydroxyl and acetyl groups. The intermolecular contacts present in the crystal structure are the C–H···O and C–H···π interactions and the π··· π stacking. The energy surface for the internal rotation about the C$_{sp2}$–O/C bonds in the khellinone and visnaginone molecules has been explored by quantum-chemical calculations. The density functional theory (DFT) methods yielded three stable conformers of khellinone and two of visnaginone obtained by a rotation of the methoxy group about the C4$_{sp2}$–OCH$_3$ bond. The most stable conformation in the gas phase is consistent with the stereochemistry of the molecules adopted in the solid. The secondary minima conformers have energies higher by 0.3–1.8 kcal/mol. The energy of the intramolecular O–H···O interactions, present in the molecular structure of all stable conformers, is around 18 kcal/mol at the DFT level. A complete and reliable assignment of the bands in the IR and Raman spectra of both compounds has been performed.

T. Pena Ruiz · M. Fernandez Gomez
Department of Physical and Analytical Chemistry,
University of Jaen, 23071 Jaen, Spain

A. Drzewiecka · A. E. Koziol (✉)
Faculty of Chemistry, Maria Curie-Sklodowska University,
23-031 Lublin, Poland
e-mail: anna.koziol@poczta.umcs.lublin.pl

A. Drzewiecka
Institute of Physics, Polish Academy of Sciences,
02-668 Warsaw, Poland

K. Ostrowska
Department of Organic Chemistry, Faculty of Pharmacy,
Medical University of Warsaw, 02-097 Warsaw, Poland

K. Ostrowska · M. Struga · J. Kossakowski
Department of Medicinal Chemistry, Faculty of Medicine I,
Medical University of Warsaw, 02-007 Warsaw, Poland

Introduction

The benzo[b]furan system, as an important pharmacophore, is present in numerous compounds which can be isolated from the natural sources, and is an essential fragment of newly synthesized pharmaceuticals (e.g., amiodarone [1] and bergapten [2]). These heterocyclic compounds show a variety of pharmacological properties and a change of their structure is useful in the search of new therapeutic agents [3, 4].

Two benzofuran derivatives, khellinone (**1**: 5-acetyl-4,7-dimethoxy-6-hydroxy-benzo[b]furan) and visnaginone (**2**: 5-acetyl-4-methoxy-6-hydroxybenzo[b]furan) (Fig. 1), are the product of the hydrolysis of khellin and visnagin, respectively. Both khellin and visnagin are the chemical constituents of *Ammi visnaga* Lam. (Apiaceae) fruits [5], and their applications in pharmacology and biomedicine have been known for long. *Ammi visnaga* (toothpick
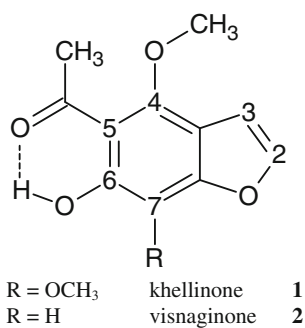
Fig. 1 Molecular formula of khellinone and visnaginone

R = OCH₃	khellinone	1
R = H	visnaginone	2

ammi), possessing the Arabic name khella and the Spanish name visnaga, has been used in the folk medicine throughout the Mediterranean countries in treating various ailments of the urinary (kidney stones) and respiratory tract (asthma) [6].

The synthetic derivatives of khellinone and visnaginone show antibacterial and antimicrobial activities [7–13], exhibit also antiarrhythmic, antiatherosclerotic, and/or cardiovascular properties [14–18], insect antifeedant activity [19], and others. Recently, it has been proved that khellinone, visnaginone, and their derivatives are able to block the Kv1.3 potassium channel with a different kind and degree of selectivity [20–26]. The Kv1.3 ion channel is involved in the pathogenesis of autoimmune diseases such as multiple sclerosis. The structure–activity relationship (SAR) and Quantitative SAR (QSAR) studies on the series of khellinone and visnaginone derivatives revealed that higher hydrophobicity improves their blocking activity.

Although the synthesis of khellinone 1 and visnaginone 2 is known for long, their molecular structures have not yet been characterized. Up to date, vibrational spectroscopic studies for khellinone and its derivatives are very scarce. Musante et al. [27] reported the infrared spectra of visnaginone and its derivatives, but without any comprehensive analysis, while Epstein et al. [28] gave a primary description of the infrared spectrum of khellinone in the region 1,180–1,020 cm⁻¹. The vibrational spectra of benzofuran itself were fully interpreted by Singh [29].

The main goal of this study is to explain how the molecular conformations depend on the methoxy substituents, and whether different conformers can be distinguished by the vibrational analysis. To compare molecular structure of the title compounds in the solid state and gas phase, an X-ray crystal structure analysis and DFT/B3LYP/B1B95 theoretical calculations were performed. Afterwards, the IR and Raman spectra were also recorded, and a reliable interpretation of the spectroscopic data has been performed by a comparison with theoretical data and scaling of the force fields.

Experimental

Synthesis of visnaginone and khellinone

The chemicals were purchased from Sigma-Aldrich and used without further purification. Khellinone 1 and visnaginone 2 were obtained by the method of Spaeth and Gruber [30, 31], i.e., by the ring-opening reactions of khellin and visnagin in the alkaline solution. Single crystals of 1 and 2 suitable for an X-ray diffraction were prepared by a slow evaporation of the solvent from an ethanolic solution at room temperature.

Table 1 Crystal data and experimental parameters for 1 and 2

Compounds	1	2
Molecular formula	$C_{12}H_{12}O_5$	$C_{11}H_{10}O_4$
Crystal system	Triclinic	Monoclinic
Space group	$P\bar{1}$	$P2_1/n$
a (Å)	7.322(1)	7.906(2)
b (Å)	8.580(1)	7.337(1)
c (Å)	9.859(1)	17.060(3)
α (°)	70.57(1)	90
β (°)	78.94(1)	102.55(3)
γ (°)	72.72(1)	90
V (Å³)	554.8(1)	965.9(3)
Z	2	4
d (g cm⁻³)	1.414	1.418
Absorption coefficient (mm⁻¹)	0.940	0.916
$F(000)$	248	432
Crystal size (mm)	0.38 × 0.15 × 0.12	0.40 × 0.19 × 0.11
θ range for data collection (°)	4.78–75.06	5.31–75.13
Index ranges	$0 \leq h \leq 9$	$-9 \leq h \leq 9$
	$-10 \leq k \leq 10$	$0 \leq k \leq 9$
	$-12 \leq l \leq 12$	$-21 \leq l \leq 0$
Reflections collected	2397	2027
Independent reflections	2211	1965
Number of parameters	157	139
Goodness-of-fit on F^2	1.043	1.046
R_1 [$I > 2\sigma(I)$]	0.0627	0.0374
wR_2 [$I > 2\sigma(I)$]	0.1808	0.1107
Largest diff. peak and hole (e Å⁻³)	0.30 and −0.27	0.22 and −0.18
CCDC No[a]	849 114	849 115

[a] Copies of the data can be obtained free of charge on application to The Director, CCDC, 12 Union Road, Cambridge CB2 1EZ, UK (http://www.ccdc.cam.ac.uk)

1 (**1a** in gas phase)   **2** (**2a** in gas phase)
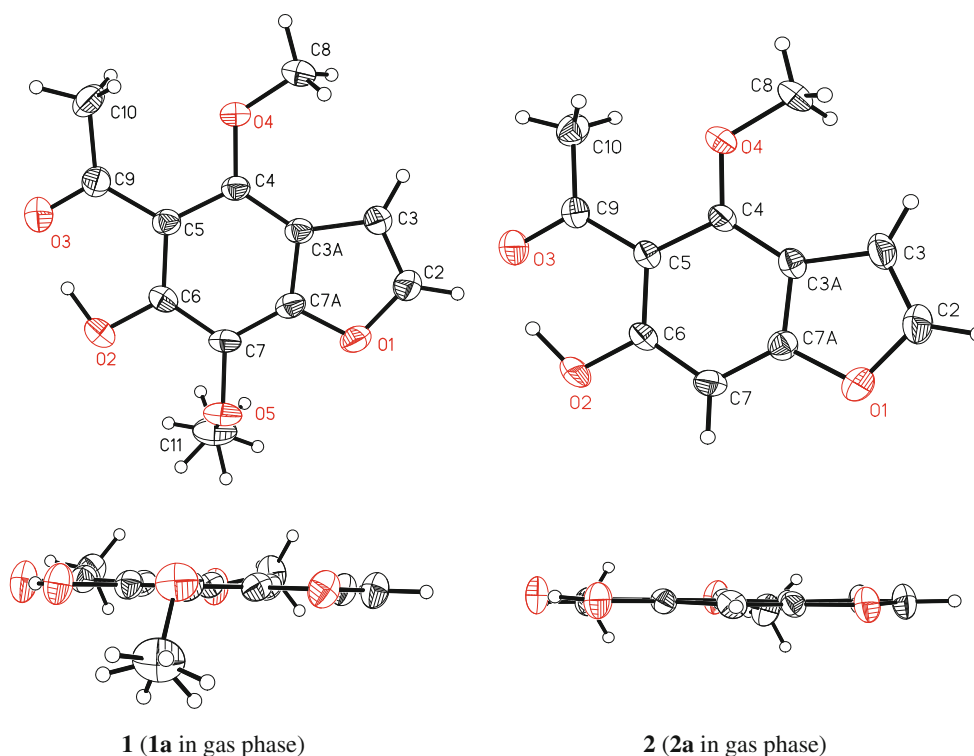
Fig. 2 Molecular structure with atom-numbering scheme of khellinone (**1**) and visnaginone (**2**). View perpendicular and parallel to benzo[b]furan system

Table 2 Selected geometric parameters of molecules **1** and **2** observed in solid state

|		**1**			**2**
Torsion angles (°)					
C6–C5–C9–O3 (acetyl group)		−5.3(4)			−4.0(2)
C11–O5–C7–C6 (methoxy group) $t1$		83.4(3)			–
C8–O4–C4–C3A (methoxy group) $t2$		−16.4(4)			−16.0(3)
Interplanar angles (°)					
Benzofuran ring/acetyl group [C5–C9(=O3)–C10]		6.6(1)			4.8(1)
Benzofuran ring/methoxy group (C4–O4–C8)		15.3(2)			15.7(2)
Benzofuran ring/methoxy group (C7–O5–C11)		82.0(3)			–
Intramolecular hydrogen-bond	D–H···A	d(D–H) (Å)	d(H···A) (Å)	d(D···A) (Å)	∠D–H···A (°)
1	O2–H2···O3	1.02	1.46	2.463(3)	165
2		1.07	1.48	2.464(2)	149

X-ray crystallography

The diffraction data were collected on an Oxford KM4 diffractometer with the Cu Kα radiation at room temperature. The structure was solved by direct methods using the SHELXS-97 program and refined by the full-matrix least-squares method on F^2 using the SHELXL-97 program [32]. The non-hydrogen atoms were refined with anisotropic displacement parameters. All carbon-bonded H-atoms were positioned geometrically and allowed to ride on the attached atom. The coordinates of the hydroxyl group H-atoms were found in the difference electron density maps and they were riding during the refinement with the fixed O–H distance. The isotropic displacement parameters of the H-atoms were $U_{iso}(H) = 1.3\ U_{eq}(C)$ for the methyl groups and $U_{iso}(H) = 1.2\ U_{eq}(C/O)$ for the rest of atoms.

Table 3 Geometry of intermolecular contacts in crystal of **1** and **2**

D–H⋯A	d(D–H) (Å)	d(H⋯A) (Å)	d(D⋯A) (Å)	∠D–H⋯A (°)	Symmetry code for A
1					
C2–H4⋯O1	0.93	2.84	3.205(3)	105	$-x, 1-y, 2-z$
C10–H102⋯O5	0.96	2.68	3.613(4)	166	$-x, 1-y, 1-z$
C8–H83⋯O2	0.96	2.77	3.378(3)	122	$x, 1+y, z$
C3–H3⋯O2	0.93	2.49	3.409(3)	172	$x, 1+y, z$
2					
C8–H8A⋯O2	0.96	2.67	3.227(2)	117	$-1/2+x, 1/2-y, -1/2+z$
C3–H3⋯O2	0.93	2.71	3.640(3)	175	$-1/2+x, 1/2-y, -1/2+z$
C2–H2⋯O3	0.93	2.56	3.426(2)	155	$1/2+x, 1/2-y, -1/2+z$
C7–H7⋯O1	0.93	2.69	3.606(2)	171	$2-x, -y, 1-z$
C10–H10C⋯Cg	0.96	2.88	3.574(3)	141	$1-x, 1-y, 1-z$

Cg centre of gravity of the benzene ring
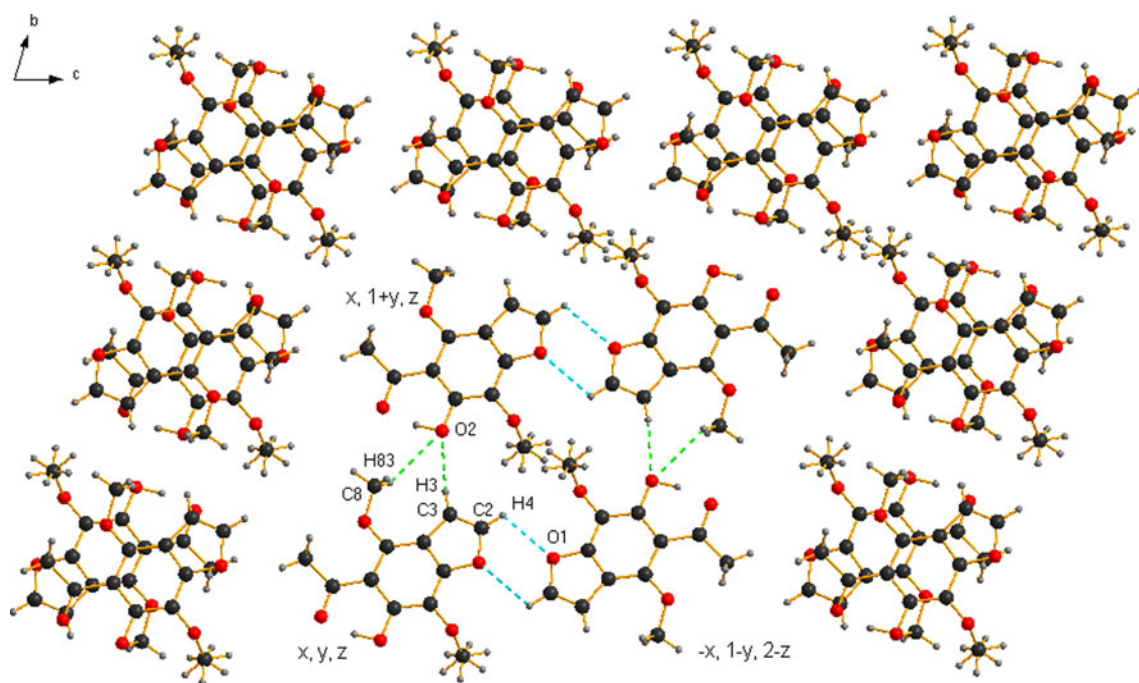

Fig. 3 Centrosymmetric tetramer and dimer of molecules present in crystal of **1**. The C–H⋯O interactions linking the molecules are shown by *broken lines*

The crystallographic data and details of the data collection and refinement are given in Table 1.

Vibrational data

The IR and Raman spectra were recorded at the resolution of 1 cm^{-1} on a Bruker FTIR Vector 22 equipped with a DTGS detector, and a Bruker FT-Raman RFS 100/S with a Nd:YAG laser emitting at 1,064 nm (laser power 500 mW) and a liquid N$_2$-cooled Ge detector. The spectra were managed by using the OPUS 2.2 package [33, 34].

The gas-phase IR spectra were recorded with a gas cell Specac 5650 (KBr windows). The solid samples were melted and evaporated at ca 10 mmHg. The best spectra were obtained at ca 205 and 190 °C for **1** and **2**, respectively. The liquid phase spectrum for **1** was recorded in the CCl$_4$ solution (Fluka 99.8%, iden. HPLC). For this measurement a liquid cell Buck Scientific (CsI windows with spacers of 0.1 and 0.2 mm) was used. The solid phase spectra for **1** and **2** were recorded in the KBr (Sigma-Aldrich +99% iden. IR) matrix.
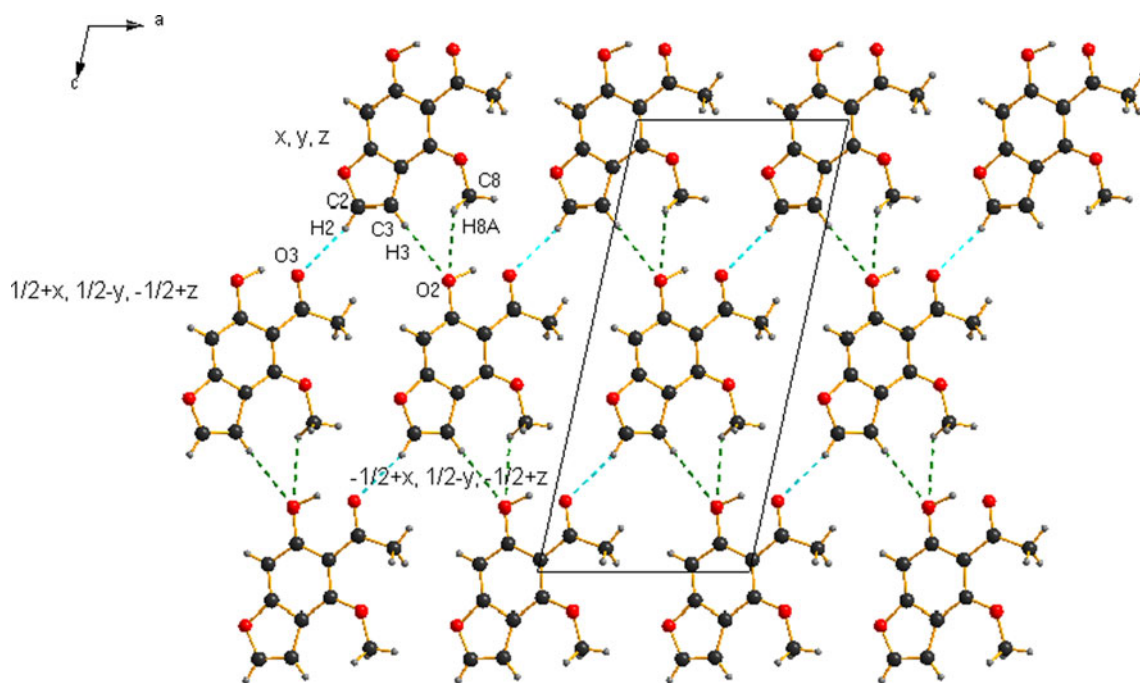
Fig. 4 Layer viewed down the *b*-axis in crystal of **2**. The C–H···O interactions linking the molecules are shown by *broken lines*

Computational details

The Gaussian 03 package [35] was used for all the theoretical calculations. The density functional theory (DFT) functionals B3LYP and B1B95 [36–38] as well as the ab-initio MP2 [39] approximation were the initial selected methods to run the simulations. The choice of those theoretical methods was based on the analysis of Riley et al. [40] who evaluated an assortment of density functionals on the calculation of bond distances, bond angles, and hydrogen bond energies. As a result, B1B95 was placed in the first position of the ranking (or second depending on the basis set) and B3LYP was classified as the sixth one (or the fifth). MP2 has been used for comparative purposes.

Further tests on the performance of these methods were conducted to reproduce the solid-state molecular conformation and the vibrational spectrum. The 6-31G(d), 6-31+G(d), 6-31+G(d,p), and 6-311++G(d,p) basis sets were implemented (Supplementary material).

The potential energy surface (PES) for the rotation of the methoxy groups in **1** and **2** was simulated with both DFT functionals and the MP2 approach along with the 6-31G(d) basis set [41–43].

The Polarizable Continuum Model within the Integral Equation Formalism Model (IEFPCM) [44] was used to simulate the most stable minima in aqueous solution.

In order to perform an adequate vibrational analysis the B3LYP/6-31G(d) force field was scaled according to Pulay's Scaled Quantum Mechanics Force Field (SQMFF)
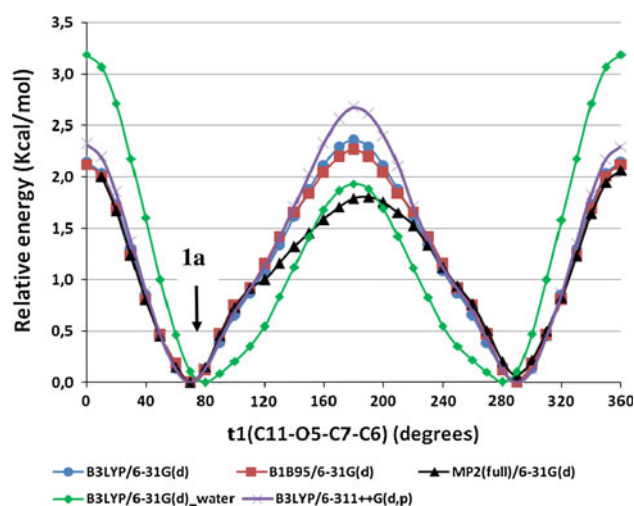
Fig. 5 Calculated energy curve of **1** for the rotation of the methoxy group around the C7–O5 bond

scheme [45, 46] using natural coordinates and MOLVIB [47, 48] code.

Finally, the intramolecular –O–H···O hydrogen bond was characterized by NBO methodology [49] and the barrier to rotation of the acetyl group. The latter parameter was estimated with both B3LYP/6-31G(d) and B3LYP/aug-cc-pVDZ//B3LYP/6-31G(d) approximations and corrected for the Basis Set Superposition Error (BSSE) [50] with Boys and Bernardi's counterpoise approach (Supplementary material).

Table 4 Torsion angles (°), $t1$ (C11–O5–C7–C6) and $t2$ (C8–O4–C4–C3A), and relative energy (kcal/mol) for conformers of **1** and **2** in gas phase calculated with different methods

Molecule	**1**			**2**	
Conformer	**1a**	**1b** (*trans*)	**1c** (*cis*)	**2a**	**2b**
Method: B3LYP/6-31G(d)					
$t1$	70.1	68.4	68.1	–	–
$t2$	−0.9	−73.1	72.4	0.0	±71.0
Relative energy	0.0	0.34	0.42	0.0	1.36
Method: B1B95/6-31G(d)					
$t1$	71.4	70.0	69.8	–	–
$t2$	−0.5	−73.6	72.8	0.0	±71.7
Relative energy	0.0	0.75	0.82	0.0	1.78
Method: MP2/6-31G(d)					
$t1$		70.0	−70.2	–	–
$t2$		−77.5	−80.0	±79.0	
Relative energy		0.0	0.07	0.0	

Results and discussion

Molecular structure in solid

The bond lengths and angles of both molecules are within the expected ranges and are equal within the experimental error. The benzo[b]furan unit is almost planar; the maximal deviations from the best-plane are observed for the C6 atom [0.012(2) and 0.025(2) Å for **1** and **2**, respectively]. The hydroxyl group of **1** and **2** is in the *ortho* position to the acetyl group (Fig. 2) and this substitution promotes formation of the stable intramolecular O–H···O hydrogen bond with the S(6) motif [51, 52] (Table 2). The dihedral angle between the plane of the acetyl group and the plane of the benzo[b]furan atoms is 6.6(1)° and 4.8(1)° for **1** and **2**, respectively.

The molecule **2** contains one methoxy group connected with the benzo[b]furan ring system, whereas the molecule of its derivative **1** has two –OCH₃ groups in the *para* position. One of these methoxy groups (at C4) is nearly coplanar with the ring; the torsion angle C8–O4–C4–C3A is −16.4(4)° and −16.0(3)° for **1** and **2**, respectively. For the methoxy group at C7, the torsion angle C11–O5–C7–C6 is 83.4(3)° (Table 2). This almost perpendicular orientation of the second –OCH₃ substituent is in good agreement with molecular conformation observed for similar benzo[b]furan derivatives [21, 53].

Crystal structure

Since the hydroxyl group of both molecules forms a strong intramolecular O–H···O hydrogen bond, other types of weak and less directional forces, such as C–H···O and C–H···π interactions, play an important role in generating the supramolecular architecture [54–57].

The structure of **1** is stabilized by the intermolecular C–H···O hydrogen bonds (Table 3). The C2–H4···O1 interactions link the molecules into the ring $R_2^2(6)$ and the "chelating" hydrogen bonds (C3–H;C8–H)···O2 connect molecules to form a centrosymmetric tetramer (Fig. 3).

The main pattern in the crystal of **2** is a folded layer (Fig. 4; Table 3) stabilized by the intermolecular C–H···O
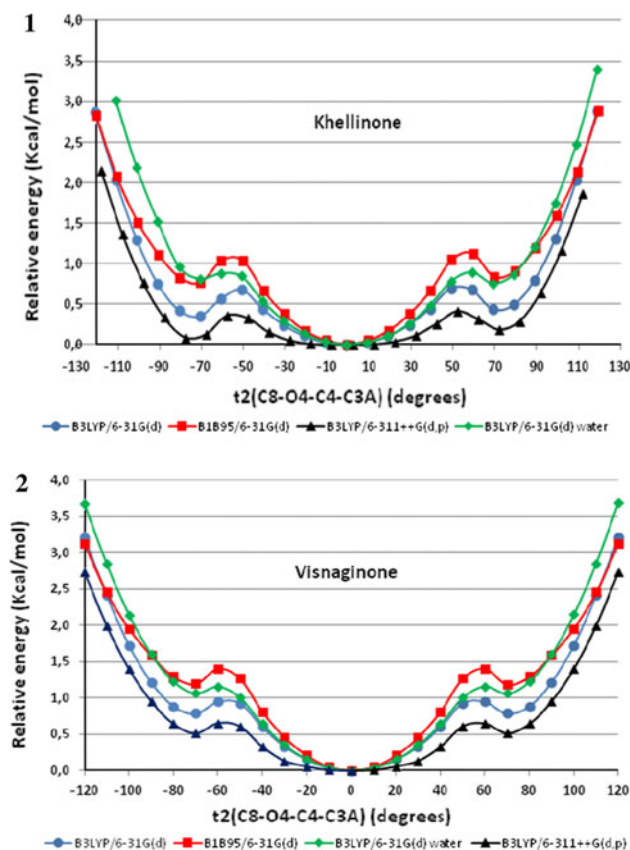
Fig. 6 Energy surface of the methoxy group rotated around the O4–C4 bond for **1** and **2**

t2=-73.1 degrees

t1=68.4 degrees

1b

t2=72.4 degrees

t1=68.1 degrees

1c
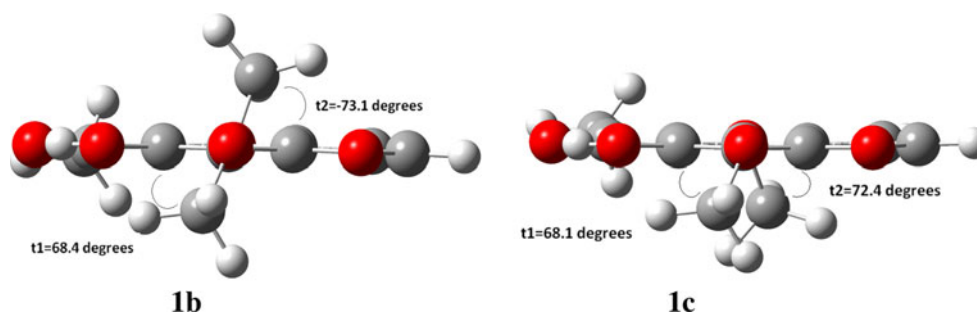
hydrogen bonds. These layers interact by the C10–H··· π contacts.

The introduction of the second methoxy group, perpendicular to the benzo[b]furan ring system in **1**, does not influence significantly the relative arrangement within the pairs of parallel molecules observed around the symmetry centers. In the crystals of **1** and **2**, the C···π distances between the parallel molecules (with the partial overlapping of the phenyl rings) are about 3.36–3.45 Å.

Conformational analysis in gas phase

The benzo[b]furan ring is rigid and the intramolecular O–H···O hydrogen bond stabilizes the orientation of the acetyl group; the theoretical approximations reveal a stabilization energy of the intramolecular O–H···O hydrogen bond around 18 kcal/mol (Supplementary material Table 1S; Fig. 1S). Thus, the search for stable conformers of the compounds **1** and **2** was focused on the rotation of their –OCH$_3$ groups. The PES for the torsion angles $t1$ (C11–O5–C7–C6; for **1** only) and $t2$ (C8–O4–C4–C3A, for both molecules) was scanned within the isolated molecule approximation.

Energy surface for (C7)–OCH$_3$ group in 1

The rotation about the C7–O5 bond, calculated by the DFT functionals with the 6-31G(d) basis set, for **1** gives one stable conformer (**1a**). The methoxy group at C7 of **1a** is almost perpendicular to the benzo[b]furan fragment ($t1$ ±70°) and the second substituent (C4)–**OCH$_3$** is coplanar to the aromatic ring (Fig. 5; Table 4). The calculated geometry of the molecule in the gas phase, **1a**, is in the agreement with its structure observed in the crystal (Fig. 2; Table 2). The barriers to torsion are in the range 2.0–2.5 kcal/mol what suggest a significant rigidity for the position of this group.

The energy profile for MP2(full)/6-31G(d) yielded different results than DFT/6-31G(d). Both methoxy groups are nearly perpendicular to the aromatic ring, giving two stable conformers, with the *trans* and the *cis* orientations of the –OCH$_3$ substituents (Table 4).

Energy surface for (C4)–OCH$_3$ groups in 1 and 2

The PES for internal rotation about the C4–O4 bond, calculated using the DFT functionals with 6-31G(d) basis set, yields three minima for both molecules (Fig. 6). In addition to **1a**, khellinone has two new conformers with the *trans* (**1b**) and *cis* (**1c**) orientations of the methoxy groups (Fig. 7; Table 4). These conformers are energetically less stable than **1a** [<0.5 kcal/mol for B3LYP/6-31G(d) and 0.9 kcal/mol for B1B95/6-31G(d)].

A similar pattern of the equivalent torsional surface is observed for visnaginone (**2**) (Fig. 6). The methoxy group of the most energetically favorable conformer **2a** is coplanar to the benzo[b]furan ring system, and this stereochemistry corresponds to that observed in the crystal (Fig. 2). The secondary minima, being the mirror images, represent the second conformer **2b** described by $t2$ ±71° (Table 4). The energy differences between the stable conformers are slightly higher for **2** than for **1**. The barriers to torsion are in the range 1.0–1.5 kcal/mol for both compounds.

The data obtained using the MP2(full)/6-31G(d) approach are different from those obtained with the DFT methods. Moreover, the MP2 method does not predict a coplanarity of the (C4)–OCH$_3$ group with the benzo[b]furan system (Table 4).

The behavior of the (C4)–OCH$_3$ group for **1** and **2** can be compared with the results established by Bzhezovskii et al. [58] for anisol and *para*-methoxyanisol. The most stable structure for the latter compounds shows the methoxy group coplanar to the benzene ring and a perpendicular conformation occurs as a less stable geometry. Both **1** and **2** show a similar energetic profile for the torsion angle $t2$. For the benzo[b]furan derivatives the secondary minima and the barriers to rotation are shifted to the lower values of $t2$, probably due to the bulky acetyl group in the *ortho* position. Analogous to

Table 5 Comparison of the experimental and calculated vibrational spectra of khellinone (**1**) and assignments

Experimental frequencies (cm^{-1})				Scaled theoretical frequencies			Assignments[a]
IR gas	IR CCl$_4$	IR solid	Raman solid	1a	1b	1c	
		3,160	3,161	3,180	3,170	3,170	C(furan)–H sym str.
		3,140	3,140	3,159	3,144	3,144	C(furan)–H asym str.
				3,039	3,044	3,043	C(CH$_3$)–H asym str.
				3,028	3,033	3,033	C(CH$_3$)–H asym str.
		3,014	3,016		3,031	3,031	O–H str[S]
2,975				3,028	3,028	3,028	C(CH$_3$)–H asym str.
				3,015	3,015	3,015	C(CH$_3$)–H asym str.
		2,989	2,991	2,993			C(CH$_3$)–H asym str.
	2,998			2,992	2,997	2,997	C(CH$_3$)–H asym str.
		2,962	2,963	2,980	2,977	2,977	O–H str.|C(CH$_3$)–H asym str.[S]
				2,949	2,949	2,949	C(CH$_3$)–H sym str.
2,939	2,936	2,933	2,933	2,922	2,917	2,915	C(CH$_3$)–H sym str.
				2,913	2,912	2,912	C(CH$_3$)–H sym str.
1,624	1,631	1,625	1,626	1,627	1,632	1,632	C=O str., rocking acetyl
		1,619		1,618	1,619	1,619	Phenyl ring str., furan ring def.
	1,582	1,586	1,587	1,590	1,593	1,592	Phenyl ring str.
		1,548	1,549	1,552	1,542	1,542	Furan ring str., C(furan)–H rocking
1,472	1,472	1,472	1,474	1,475	1,476	1,476	CH$_3$(methoxy) asym. def.
				1,475	1,473	1,473	CH$_3$(methoxy) asym. def.
			1,456	1,465	1,463	1,463	CH$_3$(methoxy) sym. def.
				1,460	1,451	1,451	CH$_3$(methoxy) asym. def.
	1,442	1,444		1,451	1,451	1,451	CH$_3$(methoxy) asym. def.
				1,440	1,442	1,442	CH$_3$(acetyl), asym. def.
				1,434	1,435	1,435	CH$_3$(methoxy) sym. def.
1,417	1,414	1,424	1,429	1,426	1,426	1,426	CH$_3$(methoxy) sym. def.
				1,422	1,420	1,420	C–O–H def., C–OH str.
				1,415	1,413	1,413	CH$_3$(acetyl), asym. def., C–O–H def.
		1,380	1,379	1,373	1,368	1,368	CH$_3$(acetyl), sym.
1,363	1,366	1,364	1,366	1,359	1,362	1,362	CH$_3$(acetyl), sym.
1,351	1,352	1,352	1,350	1,347	1,350	1,350	Benzofuran ring str.
	1,302	1,303	1,302	1,291	1,302	1,301	C–C(acetyl) str., rocking C(furan)–H
1,291	1,291			1,287	1,290	1,290	C–O(methoxy), phenyl ring str.
1,276	1,277	1,266	1,265	1,280	1,281	1,281	Phenyl ring str.
		1,212	1,211	1,212	1,200	1,199	Furan ring def., C–O(methoxy) str.
		1,199		1,199	1,194	1,194	CH$_3$(methoxy) rocking
1,170	1,172	1,171	1,177	1,180	1,171	1,172	Furan ring str.–def.
1,141	1,146	1,150	1,155	1,157	1,154	1,154	C–O(methoxy) str., CH$_3$(methoxy) rocking|CH$_3$(methoxy) rocking[S]
				1,153	1,152	1,152	C(furan)–H rocking, furan ring def.|CH$_3$(methoxy) rocking[S]
				1,152	1,148	1,148	CH$_3$(methoxy) rocking|CH$_3$(methoxy) rocking, furan ring def.[S]
				1,152	1,131	1,131	CH$_3$(methoxy) rocking|furan ring str., C(furan)–H rocking[S]
1,065	1,063	1,079	1,078	1,083	1,066	1,066	Furan ring str.|CH$_3$(acetyl) rocking, C–O methoxy str.[S]
		1,062	1,040	1,064	1,060	1,061	Furan ring str.–def.
		1,041		1,049	1,034	1,034	Furan ring str.–def.
		1,029		1,036	1,027	1,028	CH$_3$(acetyl) rocking
985	985	987	990	985	972	973	O–C(CH$_3$) str.
974	975	977	980	969	966	966	CH$_3$(acetyl) rocking, C–C(CH$_3$) str.

Table 5 continued

Experimental frequencies (cm^{-1})				Scaled theoretical frequencies			Assignments[a]
IR gas	IR CCl$_4$	IR solid	Raman solid	1a	1b	1c	
940	944	942		937	938	938	Furan ring str.–def.|O–C(CH$_3$) str., furan ring str.–def.[S]
878	878	881	881	876	874	874	Furan ring def.
843		851	847	845	845	845	Furan ring str.–def.
				836	835	835	C(furan)–H opl def.
		788	791	796	794	794	C–OH rocking, C–C(acetyl) rocking
		777	777	737	752	752	C(furan)–H opl def.
737		756	754	790	772	772	–OH torsion
694		701	690	690	715	714	C–OH opl def., phenyl ring torsion, C–OCH$_3$ opl def.
		688		685	689	689	Phenyl ring torsions
669				666	676	675	Phenyl ring torsions, C–C(acetyl) opl def., C–OCH$_3$ opl def.
633	631	638	640	633	627	631	Acetyl group def.
590	594	597	600	589	593	594	Phenyl ring def.
		589	588	577	580	578	Furan ring torsions
573	572	570	571	558	567	565	Furan ring torsions
	530	538	536	523	531	514	C–OH opl def., C–O–CH$_3$ def.
			496	483	484	489	Phenyl ring def.
	475		455	460	438	457	C–O–CH$_3$ def., C(acetyl)–C(phenyl) rocking
	440						
			419	418	416	417	C–OH rocking, C(acetyl)–C(phenyl) rocking
	385		395	398	388	394	C(acetyl)–C(phenyl) rocking, phenyl ring def.
			376	370	364	350	Phenyl ring def., C–O–CH$_3$ def.
			341	332	333	325	Phenyl ring def., C–O–CH$_3$ def.
			324	316	309	311	C(phenyl)–C(acetyl) opl def., butterfly
			280	284	292	295	C–OCH$_3$ rocking, phenyl ring def.
				277	272	267	CH$_3$(methoxy) rotation
			260	266	246	247	Acetyl group rocking
				242	227	230	C–OCH$_3$ rocking
				233	200	202	CH$_3$(acetyl) rotation
				222	173	173	Acetyl group rocking, C–O–CH$_3$ def.
			206	191	153	155	Phenyl ring torsions, butterfly
			175	162	138	138	Phenyl ring torsions, –OH torsion
			125	138	133	132	CH$_3$(methoxy) rotation
			105	104	100	100	–OH torsion, acetyl group torsion
			83	79	91	92	CH$_3$(methoxy) torsion, phenyl ring torsions
				64	70	69	CH$_3$(methoxy) torsion
				39	62	62	Acetyl group torsion, CH$_3$(methoxy) torsion
				30	41	41	CH$_3$(methoxy) rotation

str. stretching, *def.* deforming, *opl* out of plane deformations

[a] Description of normal modes is based on the potential energy distribution matrix for the most stable conformer **1a**. Description of modes for the secondary minima, **1b** and **1c**, has been also included for bands interesting for the conformational analysis when a significant difference respect to **1a** is expected

The symbol "|" and superindex "S" indicate that the description corresponds to the secondary minima

the conformers of anisol and *para*-methoxyanisol [58], the second *para*-methoxy group in the conformers of **1** is responsible for the smaller torsional barrier and lower relative energy than those observed for **2**.

Conformational analysis in liquid phase

As **1** and **2** show their action in aqueous cellular media, the energy surfaces were explored by changing the torsion

Fig. 8 *Left column* IR spectra in the range 1,250–1,000 cm^{-1} for **1**. *Right column* second derivative. **a** Gas phase; **b** *black solid line* CCl$_4$ solution of **1**, *red dashed line* CCl$_4$; **c** solid phase; **d** *black solid line* conformer **1a**, *red dashed dotted line* conformer **1b**, *blue dotted line* conformer **1c** (Color figure online)
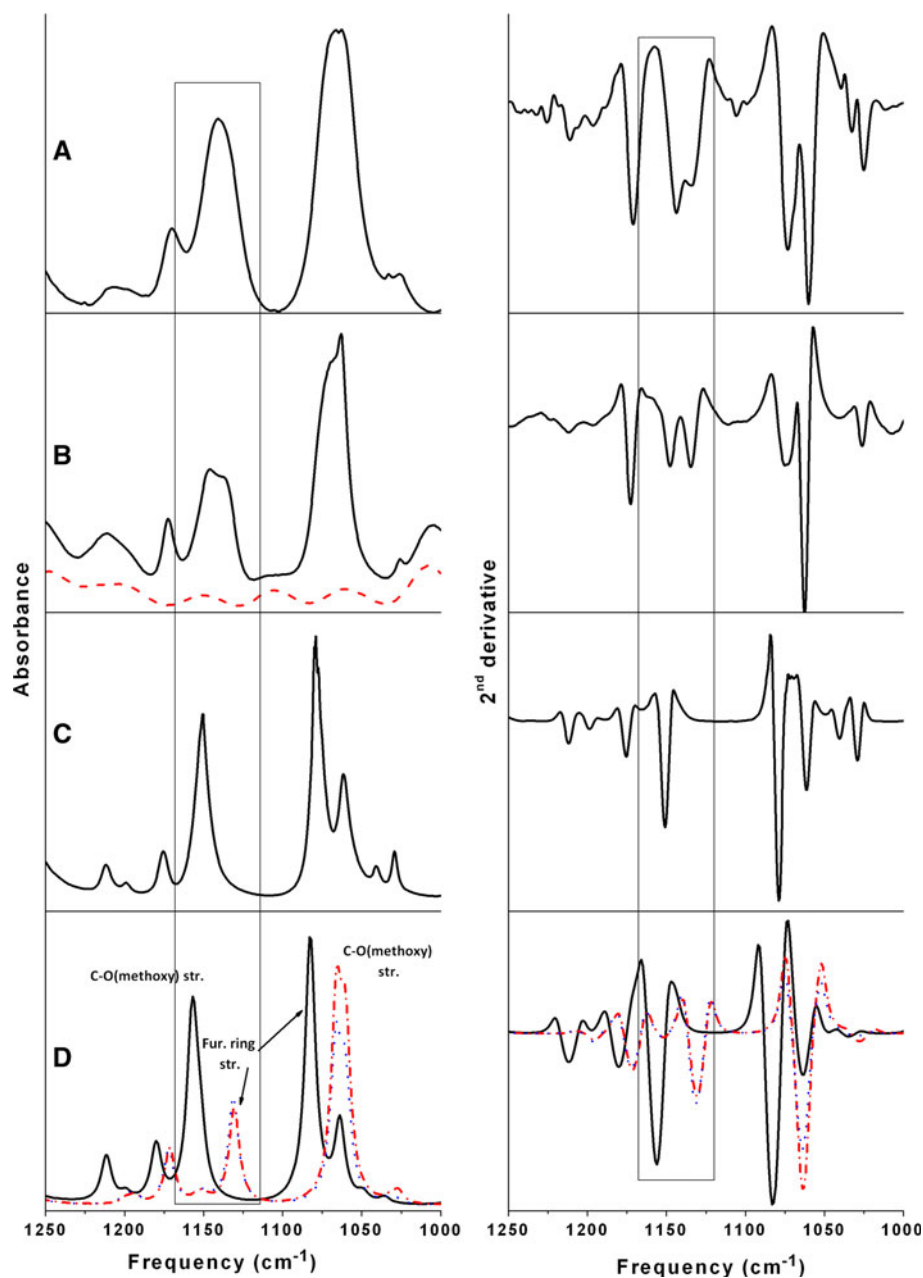
angles *t*1 and *t*2 in an aqueous solution; B3LYP/6-31G(d) was the method of choice. The internal rotation around the **C7–OCH$_3$** single bond for **1** yielded two mirror images (analogous to those obtained for the isolated molecule) with the methoxy group at the C7 atom almost perpendicular to the benzo[b]furan fragment (*t*1 is shifted to ±80°) (Fig. 5). The PES for the internal rotation about the C4–O4 single bond yields also three minima for both molecules (Fig. 6). However, the secondary minima for **1** and **2** almost disappear and their relative energy to the most stable conformer increases (Fig. 6).

Vibrational analysis

The discussion is focussed on the region of spectra from 1,250 to 1,000 cm^{-1} to support the previous conformational analysis. Since the low barriers to rotation result in the overlapping of bands of different conformers, the second derivative of the spectrum was used to reveal peaks under the broad bands.

The full assignment of the vibrational spectra for **1** is presented in Table 5, and for **2** is reported as Supplementary material (Table 2S).

On the spectrum of **1** in the region 1,250–1,000 cm^{-1} (Fig. 8) an evidence for the existence of several conformers appears. Thus, two different scaled theoretical bands for the conformers **1a** and **1b/1c** appear at 1,157 cm^{-1} (**1a**, C–O stretching of the methoxy groups) and 1,131 cm^{-1} (**1b/1c**, furan ring stretching), respectively (Fig. 8d).This couple corresponds to a broad band appearing in the gas phase at 1,141 cm^{-1} and at 1,146 cm^{-1} in the CCl$_4$ solution (Fig. 8a, b, respectively). Both broad bands of the IR spectra split into two peaks in the second derivative that match the two corresponding bands of the scaled theoretical spectrum (Fig. 8d). This splitting is more visible in the spectrum of the CCl$_4$ solution than in the gas phase which is consistent with the temperature of recording; the first spectrum was recorded at room temperature and the latter at 205 °C. In the solid phase a sharpened band is observed at 1,150 cm^{-1} (Fig. 8c). The second derivative of the IR spectrum in the solid phase, where only one conformer is present, confirms the presence of one single band.

Other regions of the spectra show no significant evidences to support the conformational equilibrium. The region of the X–H stretching could be interesting because the scaled theoretical spectra reveal a clear difference among the O–H stretching bands of the conformers **1a** and **1b/1c**. In the gas phase and the CCl$_4$ solution broad bands are observed, and—as a consequence of this—the large number of bands appear in the second derivative which prevent unequivocal interpretation of results.

For visnaginone (**2**), less visible evidences are observed in the same region of the respective spectra, nevertheless they are conclusive. Two IR scaled theoretical bands appear at 1,105/1,078 cm^{-1} (furan ring deformations, O–CH$_3$ stretching) for **2a** and **2b**, respectively (Fig. 3S,C). In the IR gas-phase spectrum of **2**, the broad band at 1,091 cm^{-1} corresponds to the respective theoretical bands (Fig. 3S,A). The second derivative of that spectrum reveals a band and a shoulder at lower frequency that match the scaled theoretical bands (Fig. 3S,A). The IR spectrum in the solid phase, where only one conformer is present, shows the sharpened band (1,107 cm^{-1}, Fig. 3S,B) that it is consistent with the second derivative of the IR spectrum. However, it was impossible to record a reasonable liquid phase IR spectra for **2** due to its low solubility in different solvents.

Conclusions

The benzo[b]furan system, as a central part of the khellinone (**1**) and visnaginone (**2**) molecules, is nearly planar. The hydroxyl and acetyl groups, being in the *ortho* position, are coplanar with the aromatic ring. The formation of the intramolecular O–H$_{hydroxyl}$···O$_{acetyl}$ hydrogen bond in all three states of matter—solid, liquid, and gas phase—is observed. The presence of this intramolecular bond in the form of six-membered ring is energetically favorable for the molecules, its strength is around 18 kcal/mol.

For both molecules several conformers are observed, they differ in the orientation of methoxy groups. For the energetically favorable forms, **1a** and **2a**, representative for the solid phase, the –OCH$_3$ substituent is coplanar to the benzo[b]furan system. In the gas phase, this group can be also perpendicular to the benzene ring. The introduction of the second *para*-substituted methoxy group (in **1**) creates a conformer for which one –OCH$_3$ group is perpendicular and the second one coplanar to the benzo[b]furan moiety. Thus, in the gas phase, apart from conformer **1a**, two other conformers were identified in which the C$_{sp2}$–O-CH$_3$ bonds are in the *trans* and the *cis* orientations (the conformers **1b** and **1c**).

The vibrational spectroscopy is a good technique to study a conformational equilibrium. In case of khellinone (**1**), the second derivative of the IR spectra (in the region 1,250–1,000 cm^{-1}), in the gas phase and the CCl$_4$ solution, provide evidences of the conformational equilibrium as compared to the solid-phase spectrum and the scaled theoretical ones of the different conformers.

Supplementary material

Data on detailed characterization of the intramolecular O–H...O hydrogen bond, the fullassignment of vibrational spectra for **2**, and optimized geometry of the most stable conformersof **1** and **2** are included as electronic supplement (14 pages).

References

1. Gill J, Heel RC, Fittin A (1992) Drugs 43:69
2. Tanew A, Ortel B, Rappersberger K, Honigsmann H (1988) J Am Acad Dermatol 18:333
3. Courchesne WE, Hejchman E, Maciejewska D, Kossakowski J, Ostrowska K (2009) Patent Application US/2009/0270496
4. Kaltenbronn JS, Quin J III, Reisdorph BR, Klutchko S, Reynolds EE, Welch KM, Flynn MA, Doherty AM (1997) Eur J Med Chem 32:425

5. WHO (2007) Monographs on selected medicinal plants, vol 3. WHO, Geneva, pp 23–32
6. Quimby MW (1953) Econ Bot 7:89
7. El-Shihi TH, Latif NAA, El-Sawy ER (2005) Egypt J Chem 48:365
8. Mandour AH, Abu-Mustafa EA, Nehad-Ahmed A, El-Bazza ZE (1994) Al-Azhar Bull Sci 5:983
9. El-Ebrashi NMA, Gohar AKMN, Nasef AMM, Khodeir MNM, El-Diwani HIA (1986) Egypt J Pharm Sci 26:261
10. Hishmat OH, El-Ebrashi NMA, Shalash MR, Ismail I (1979) Arzneimittel-Forsch 29:1081
11. Ismail E, Tawfik AA, El-Ebrashi NMA (1977) Arzneimittel-Forsch 27:1393
12. Hishmat OH, El Ebrashi NMA (1974) Indian J Chem 12:1052
13. Hafez OMA, Ahmed KM, Mandour AM, El-Khrisy EAM (1990) Pak J Sci Ind Res 33:197
14. Ragab FA, Tawfeek H (1987) Eur J Med Chem 22:265
15. Bourgery G, Dostert P, Lacour A, Langlois M, Pourrias B, Tisne-Versailles J (1981) J Med Chem 24:159
16. Gammill RB, Bell FP, Bell LT, Bisaha SN, Wilson GJ (1990) J Med Chem 33:2685
17. Schlecker R, Raschack MG, Gries J (1991) Patent US 5039701
18. Yamashita A (1986) Patent US 4623737
19. Luthria DL, Ramakrishman V, Banerji A (1993) J Nat Prod 56:671
20. Baell JB, Gable RW, Harvey AJ, Toovey N, Herzog T, Haensel W, Wulff H, Hall E (2004) J Med Chem 47:2326
21. Harvey AJ, Baell JB, Toovey N, Homerick D, Wulff H (2006) J Med Chem 49:1433
22. Bohuslavizki KH, Haensel W, Kneip A, Koppenhoefer E, Reimers A, Sanmann K (1993) Gen Physiol Biophys 12:293
23. Baell JB, Gable RW, Harvey AJ (2004) Acta Cryst E 60:o996
24. Cianci J, Baell JB, Flynn BL, Gable RW, Mould JA, Paul D, Harvey A (2008) J Bio Med Chem Lett 18:2055
25. Kumar Satuluri VSA, Seelam J, Gupta SP (2008) Med Chem 5:87
26. Saina L, Gupta SP, Kumar Satuluri VSA (2009) Med Chem 5:570
27. Musante C, Fabbrini L, Franchi A (1962) Farmaco Sci 17:520
28. Epstein WW, Horton WJ, Lin CT (1965) J Org Chem 30:1246
29. Singh VB (2006) Spectrochim Acta A 65:1125
30. Spaeth E, Gruber W (1938) Chem Ber 71:106
31. Spaeth E, Gruber W (1941) Chem Ber 74:1492
32. Sheldrick GM (2008) Acta Cryst A 64:112
33. OPUS Ver 20 (1995) Bruker Analytische Messtechnik GmbH, Karlsruhe, Germany
34. OPUS Ver 22 Suppl (1996) Bruker Analytische Messtechnick GmbH, Karlsruhe, Germany
35. Frisch MJ, Trucks GW, Schlegel HB, Scuseria GE, Robb MA, Cheeseman JR, Montgomery JA Jr, Vreven T, Kudin KN, Burant JC, Millam JM, Iyengar SS, Tomasi J, Barone V, Mennucci B, Cossi M, Scalmani G, Rega N, Petersson GA, Nakatsuji H, Hada M, Ehara M, Toyota K, Fukuda R, Hasegawa J, Ishida M, Nakajima T, Honda Y, Kitao O, Nakai H, Klene M, Li X, Knox JE, Hratchian HP, Cross JB, Bakken V, Adamo C, Jaramillo J, Gomperts R, Stratmann RE, Yazyev O, Austin AJ, Cammi R, Pomelli C, Ochterski JW, Ayala PY, Morokuma K, Voth GA, Salvador P, Dannenberg JJ, Zakrzewski VG, Dapprich S, Daniels AD, Strain MC, Farkas O, Malick DK, Rabuck AD, Raghavachari K, Foresman JB, Ortiz JV, Cui Q, Baboul AG, Clifford S, Cioslowski J, Stefanov BB, Liu G, Liashenko A, Piskorz P, Komaromi I, Martin RL, Fox DJ, Keith T, Al-Laham MA, Peng CY, Nanayakkara A, Challacombe M, Gill PMW, Johnson B, Chen W, Wong MW, Gonzalez C, Pople JA (2004) Gaussian, Gaussian 03. Revision C01, Inc., Wallingford
36. Becke AD (1993) J Chem Phys 98:5648
37. Becke AD (1996) J Chem Phys 104:1040
38. Lee C, Yang W, Parr RG (1988) Phys Rev B 37:785
39. Head-Gordon M, Pople JA, Frisch MJ (1988) Chem Phys Lett 153:503
40. Riley KE, Op't Holt BT, Merz KM (2007) J Chem Theory Comput 3:407
41. Ditchfield R, Hehre WJ, Pople JA (1971) J Chem Phys 54:724
42. Frisch MJ, Pople JA, Binkley JS (1984) J Chem Phys 80:3265
43. De Oliveira MA, Dos Santos HF, De Almeida WB (2000) Phys Chem Chem Phys 2:3373
44. Cances MT, Mennucci B, Tomasi J (1997) J Chem Phys 107:3032
45. Pulay P, Fogarasi G, Pongor G, Boggs JE, Vargha A (1983) J Am Chem Soc 101:7037
46. Pulay P (1995) J Mol Struct 347:293
47. Sundius T (1990) J Mol Struct 218:321
48. Sundius T (1991) MOLVIB: A Program for Harmonic Force Field Calculations, QCPE program No 604
49. Glendening ED, Reed AE, Carpenter JE, Weinhold F (2001) NBO Version 31. Theoretical Chemistry Institute, University of Wisconsin, Madison
50. Simon S, Duran M, Dannenberg J (1996) J Chem Phys 105:11024
51. Etter MC (1990) Acc Chem Res 23:120
52. Etter MC, MacDonald JC, Bernstein J (1990) Acta Cryst B46:B256
53. Baell JB, Gable RW, Harvey AJ (2003) Acta Cryst E59:o395
54. Desiraju GR, Steiner T (1999) The weak hydrogen bond in structural chemistry and biology. Oxford University Press, Oxford
55. Nishio M, Umezawa Y, Hirota M, Takeuchi Y (1995) Tetrahedron 51:8665
56. Umezawa Y, Tsuboyama S, Honda K, Uzawa J, Nishio M (1998) Bull Chem Soc Jpn 71:1207
57. Yilmaz VT, Kazak C, Kirilmis C, Kocac M, Heinemannd FW (2005) Acta Cryst C 61:o438
58. Bzhezovskii VM, Kapustin EG, Il'chenko NN (2003) Russ J Gen Chem 73:1585